

Light Flapping Micro Aerial Vehicle Using Electrical-Discharge Wire-Cutting Technique

Lung-Jieh Yang,* Cheng-Kuei Hsu,[†] and Hsieh-Cheng Han[‡]
Tamkang University, Tamsui 251, Taiwan, Republic of China
and
Jr-Ming Miao[§]
National Pingtung University of Science and Technology,
Pingtung 912, Taiwan, Republic of China

DOI: 10.2514/1.38862

Electrical-discharge wire cutting is a promising technique that provides flexibility and lightness for a flapping micro aerial vehicle. Electrical-discharge wire cutting is used to fabricate the high-aspect-ratio structure of the four-bar linkage gear transmission module made of aluminum-alloy 7075. Aluminum-alloy 7075 has excellent specific strength (yield strength/density) good for durability of the transmission module in a micro aerial vehicle's tuff operation. A new flapping micro aerial vehicle of 21.6 cm wing span consequently has a minimum body mass of 5.9 g after installing the transmission module and a flexible wing frame made of carbon fibers and polyethylene terephthalate film. This micro aerial vehicle can endure a flight time of 6 min 7 s with the wingbeat frequency of 10–20 Hz. The lift and thrust coefficients of the micro aerial vehicle have been investigated through wind-tunnel testing. The proposed flapping micro aerial vehicle also exhibits the improved characteristic in the scaling law with respect to wingbeat frequency versus body mass.

Nomenclature

a	=	first linkage length of the gear transmission module
b	=	wing span or the second linkage length of the gear transmission module
C_L	=	lift coefficient, $L/(\rho U^2 S/2)$
C_T	=	(net) thrust coefficient, $(T - D)/(\rho U^2 S/2)$
c	=	third linkage length of the gear transmission module
D	=	drag
h	=	height of the holding case of the gear transmission module
J	=	advanced ratio, $U/b\omega\phi$
L	=	lift
M	=	body mass
S	=	wing area
T	=	thrust
U	=	freestream velocity
w	=	width of the gear transmission gear module
ϕ	=	flapping stroke angle
ρ	=	air density
ψ	=	asymmetry angle between the second the third linkages
ω	=	flapping frequency or wingbeat frequency

I. Introduction

FLAPPING flight has been a subject of academic interest for at least a half century, and in recent years it has attracted more

attention. In 1996, Defense Advanced Research Projects Agency (DARPA) funded a three-year micro aerial vehicle (MAV) program. This program is to inspire and to create artificial flyers less than 15 cm long for military surveillance. Most of them at that time were categorized as fixed-wing or rotary-wing designs [1]. Several groups therefore developed their versions of MAVs with different configurations and actuation principles. For example, in 2001, California Institute of Technology (Caltech) created "Microbat" with a flight record of 6 min [2]. Their method uses microelectromechanical systems technology and incorporation of titanium-parylene wing. In 2005, the Technical University of Delft announced the successful hovering "Delfly," which is composed of a pair of dragon-flylike flexible wings [3]. Furthermore, in 2003, the U.S. Naval Graduate School made a fixed-wing-type MAV with a scissorlike clapping tail thruster [4]. It coins the term "flapping-wing propulsor" named by Rozhdestvensky and Ryzhov [5]. The flapping-wing propulsor demonstrated a long endurance of 20 min. Comparably, in 2005, the University of Delaware employed a 5-bar mechanism for generating a prescribed wing motion taken from hawk moth kinematic flight data by Banala et al. [6]. Another example, a mechanism for biaxial rotation of a wing for a hovering MAV was designed in 2006 by McIntosh et al. [7]. An insectlike flapping-wing mechanism was proposed by Żbikowski et al. [8,9] of Cranfield University through the novel idea of a double spherical Scotch yoke in 2005. Yang et al. [10] at Tamkang University also presented a MAV capable of exporting the onsite lift information through its polyvinylidene-fluoride-parylene composite wing in 2007.

Even though many of the aforementioned examples are successful, their flow conditions are still unsteady. An approach to this problem is to adapt the kinematics motion of natural flyers documented [11–14]. Many of the developed models mimic the wingbeat frequency, wing span, or wing loading of a bird's wing and people summarized them to the corresponding scaling laws. This information is very useful as a guideline serving the next generation of MAVs. For instance, Ho et al. [15] used Norberg [16], Greenewalt [17], and Shyy et al.'s work [18], which documented the scaling laws of birds. They quoted the wingbeat-frequency data of birds versus body mass and mentioned two aerodynamic and structural physical reasons or limits [19,20] clarifying the data deviation from a scaling law for flapping flyers, which is shown in Fig. 1. To design a smaller

Received 31 May 2008; accepted for publication 3 August 2009.
Copyright © 2009 by the American Institute of Aeronautics and Astronautics, Inc. All rights reserved. Copies of this paper may be made for personal or internal use, on condition that the copier pay the \$10.00 per-copy fee to the Copyright Clearance Center, Inc., 222 Rosewood Drive, Danvers, MA 01923; include the code 0021-8669/09 and \$10.00 in correspondence with the CCC.

*Professor, Department of Mechanical and Electromechanical Engineering, Tamkang University, 151, Ying-Chuan Road; Ljyang@mail.tku.edu.tw. Member AIAA.

[†]Specialist; currently Postdoctoral Researcher, Department of Mechanical and Materials Engineering, Wright State University, Dayton, Ohio 45435.

[‡]Postdoctoral Researcher, Department of Mechanical and Electromechanical Engineering.

[§]Professor, Department of Material Engineering, 1 Shuefu Road. Member AIAA.

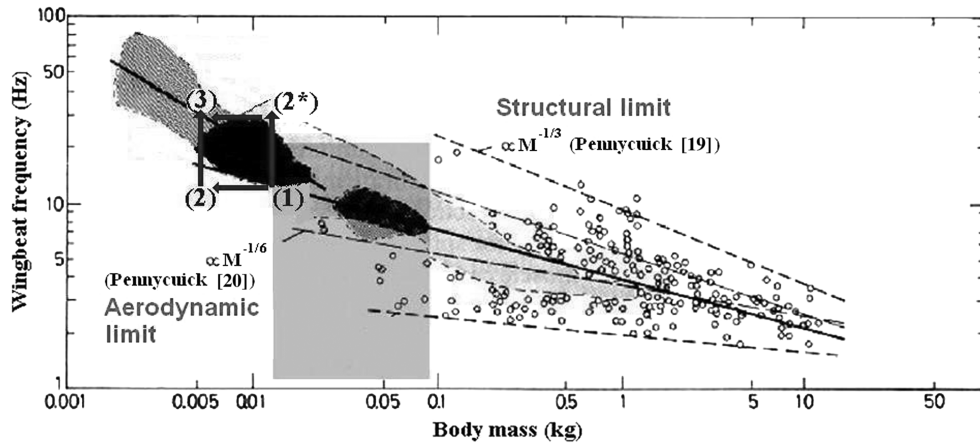


Fig. 1 Developing strategy pathways for flapping MAVs from the aspect of wingbeat frequency (see [15–20]).

and lighter MAV, there are two limits to keep in mind: one is the structural limit ($M^{-1/3}$ power law [19]) and the other is the aerodynamic limit ($M^{-1/6}$ power law [20]).

Point 2 in Fig. 1 is near to the aerodynamic limit and point 2* is near to the structural limit. Given a certain wingbeat frequency, the aerodynamic limit of Fig. 1 represents the fact that lift force cannot afford the body weight due to wingbeat frequency that is too small. Meanwhile, the structural limit in Fig. 1 represents that the structural strength is not enough to resist the high-frequency wingbeating of the flying object, given a certain body mass [15].

These two technical considerations also imply two developing strategies or pathways for delivering new generations of flapping MAVs. As depicted in Fig. 1, one could follow the pathway $1 \rightarrow 2^* \rightarrow 3$, that is, shrinking the size or increasing the wingbeat frequency of MAVs at first, to achieve the miniaturization goal if his/her expertise in handling unsteady aerodynamics is elegant. Alternatively, one had better choose the pathway $1 \rightarrow 2 \rightarrow 3$, that is, reduce the body mass of MAVs at first, if his/her key know-how is focusing on various kinds of engineering materials and processing techniques.

In this work toward the ongoing miniaturization of artificial flapping flyers, the authors prefer to choose the developing path way of $1 \rightarrow 2 \rightarrow 3$, as indicated in Fig. 1. To approach this developing path, proper material selection and design fabrication becomes the key.

II. Construction of Micro Air Vehicles

A. Micro Air Vehicle Eagle II

The very beginning of the flying model in this work is called “Eagle II” and was described in the previous work of the authors [21]. Its dimensional specifications are as follows: wing span = 30 cm, body mass = 11 g. The recorded flight time is 11 s. This MAV provides more excess length of wing span than DARPA’s requirement. Therefore, according to Norberg’s scaling law of a bird [16], the design of 20 cm wing span as well as the body mass of 10 g needs to be achieved.

The key modification of the current MAV involved the reconstruction of the four-bar linkage transmission mechanism. This transmission mechanism comes with only 1 degree-of-freedom for the flapping motion. Figure 2 shows the three-dimensional cartoons of the flapping MAV, and Fig. 3 shows the four-bar linkage module of the MAVs used in this study. In the flight transmission gear of Fig. 3a, the number 1 denotes the holding case or base, numbers 2, 3, and 4 denote the speed-reduction gears, and numbers 5 and 6 denote the second and third linkage bars. The leading-edge spar of the wing frame would be connected to the number 6 bar. The authors used 6-mm-diam Didel electric motors¹ to drive the gear transmission

module. The motor is powered by a commercial polyolithium battery (30–50 mA-hr.) The gear reduction ratio of 26.6 is designed for providing sufficient torque for actuating the flapping wing. The whole gear set and the motor were arranged originally on a polyoxymethylene (POM) holding case for Eagle II. The driving linkage made of bamboo and balsa wood controls the rotation and the follow-up linkage controls the wing beating as well. The original weight of the transmission module for Eagle II is 3.756 g.

B. Material and Fabrication Modification of Micro Aerial Vehicles

The previous work of the authors [21] has demonstrated the material disadvantage of the MAV Eagle II. It is necessary to find a new material and its corresponding processing method that can provide reliability and durability for withstanding the standard mechanical testing of MAVs. The authors select aluminum-alloy 7075 as the main structure material for the gear transmission module. Aluminum-alloy 7075 is well-known as the popular structure material applied to wings and fuselages of aircraft. Refer to the comparison of mechanical properties of 7075** to other aluminum alloys or polymers (e.g., 6061, 6063, 2024, POM, etc.), the authors can conclude that 7075 has the highest value of specific strength (density = 2.73 g/cm³, yield strength = 145–476 MPa). In other words, 7075 is a lightweight material and provides enough mechanical strength for MAVs.

About the corresponding machining of 7075 into small parts, including the motor holding case and linkage bars in this work, some considerations are addressed: Unlike plastics or other metals, aluminum alloy is ductile and hard to be joined by welding. Therefore, each moving part should be machined into a whole as far as possible. Moreover, high-aspect-ratio configuration of the small parts in Fig. 3a is desirable for providing better mechanical strength. Therefore, electrical-discharge wire cutting (EDWC) technique is chosen to construct an aluminum-alloy four-bar linkage transmission module for the MAV herein.

C. Design of the Transmission Module

The dimensional parameters of the aluminum-alloy transmission module are shown in Fig. 3c. The **a**, **b**, **c** symbols on the figure denote the lengths of the first, second, and third bars, respectively, of the four-bar linkage. The **w** and **h** symbols denote the width and the height of the module. The width is designed as 24 mm in Eagle II, but as 20 mm and 16 mm in the modified “Golden Snitch” MAV (mentioned in the next subsection). With different values of **a**, **b**, and **c**, one can control the mechanism output of flapping stroke angle and the phase lag of the two wings according to the following design rules:

¹Data available at <http://www.didel.com>.

^{**}Data available at http://en.wikipedia.org/wiki/7075_aluminium_alloy.

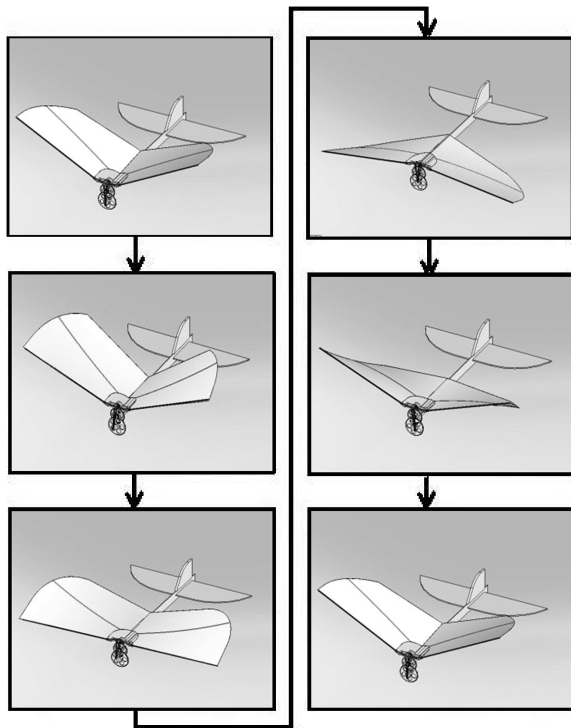


Fig. 2 Illustration cartoon of the continuous full-cycle flapping of the MAVs.

1) The length of the first bar **a** influences the flapping stroke angle and the phase lag of the two wings.

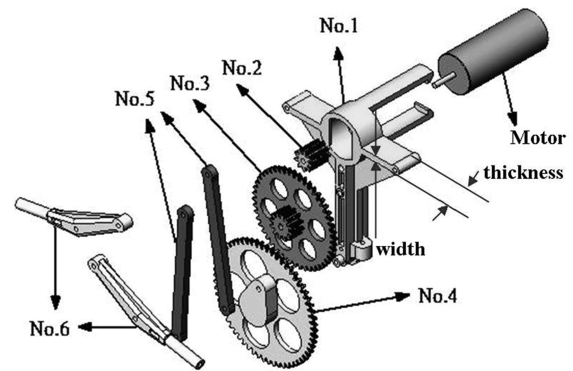
2) The length of the second bar **b** alters the flapping symmetry ϕ and the fluttering vibration during the operation. The key is dependent on the asymmetry angle of ψ between the second and the third bars, as indicated in Fig. 3b. According to the authors' experience, ψ should be kept below 30 deg to ensure the smooth operation of the transmission module.

3) The length of the third bar **c** also influences the stroke angle and the flapping symmetry. The length has to be less than $0.5w$ to avoid the collision of the linkage components during the operation.

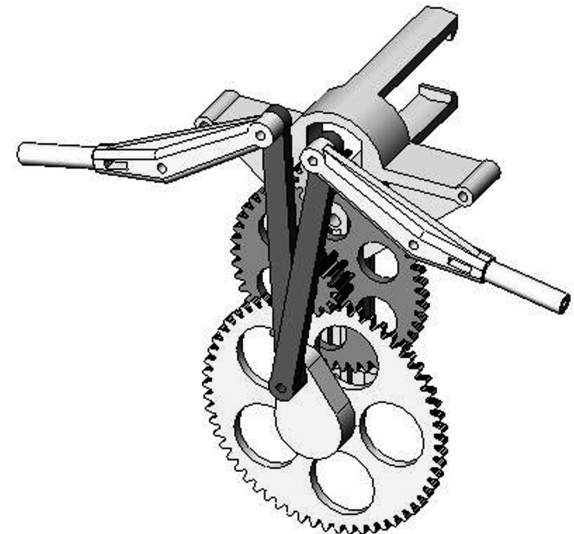
For example, a possible design can be achieved with the holding base with $w = 20$ mm, and the flapping stroke angle ϕ of 38.9 deg. The linkage bars **a**, **b**, and **c** are set as 3, 21, and 9 mm, respectively, even though there is a phase lag of 2 deg. Other possible designs for transmission modules with two groups dependent on **b** are listed in Table 1. (The mechanism analysis of the 4 bar linkage transmission module is not shown here.)

The cases of large stroke angle near 90 deg in group 2 of Table 1 fail due to mechanism stuck. The phase lag larger than 5.2 deg deduced by large stroke angle ($\phi > 70.6$ deg) deteriorates the total lift of MAVs. Moreover, the asymmetry angle ψ in Fig. 3c has influence as well, because the whole mechanism might flutter or get stuck as $\psi > 30$ deg. The resulting fluttering vibration subject to $\phi = 70.6$ deg during the operation of the transmission module generates more energy dissipation and it needs more powerful (and heavier) driving motors. This is, of course, against the miniaturization trend of MAVs. On the other hand, the designs in group 1 of Table 1 are more feasible for realization. Conclusively, the flapping stroke angle for the MAV in this study is recommended from 38.9 to 56.3 deg. This range of the flapping stroke angle ϕ is smaller than 70 deg of birds or 120 deg of hummingbirds [16].

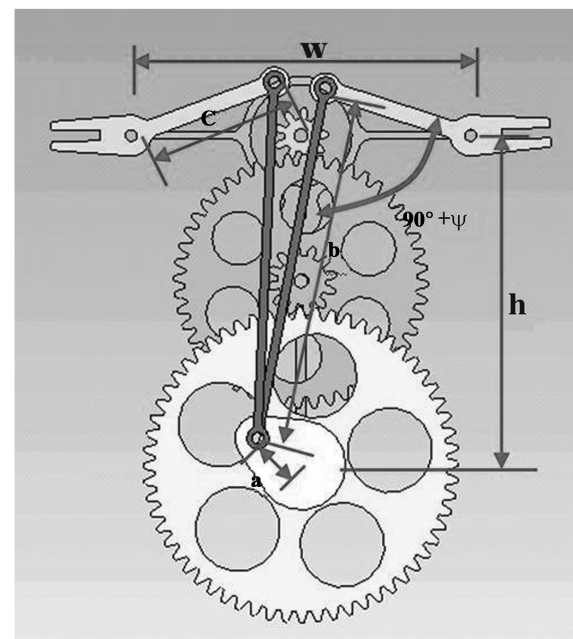
As shown in Fig. 3c, the first bar is designed to be embedded or fitted onto gear 4. The second bar is very slender. The end portion of the third bar is designed to look like a fork, so that it can be connected to the leading-edge frame. The leading-edge spar is made of carbon-fiber rod, and it makes the flapping wing firm. Additionally, the third bar is designed with a dihedral angle of 20 deg. This angle lies between the fork end and the pin joint that connects to the second bar to prevent the unstable behavior of the transmission module. The



a) The parts [21]



b) The whole gear transmission module [21]



c) The design parameters

Fig. 3 MAV with a gear transmission module of four-bar linkage.

Table 1 Some possible designs of linkage dimension for transmission modules

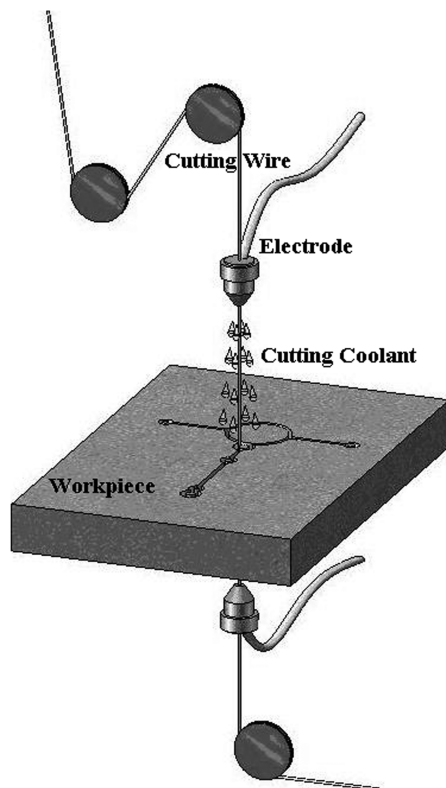
Group	b, second bar, mm	a, first bar, mm	c, third bar, mm	Holder width w, mm	Flapping stroke angle, ϕ , deg	Phase-lag angle, deg	Asymmetry angle, ψ , deg
1	21	3	9	20	38.9	2	21.2
	21	3.3	9	20	43	2.2	23.4
	21	3.65	9	20	47.9	2.6	26.5
	21	3	7	16	50.8	2.7	25.4
	21	3.3	7	16	56.3	3.2	28.7
2	20.3	2.4	9	20	30.9	1.6	14.9
	20.3	4	9	20	52.8	3.2	28.4
	20.3	5.2	9	20	70.6	5.2	40.5, fluttering
	20.3	6.3	9	20	89.4	7.9	54.6, get stuck
	20	4.9	7	16	89.2	6.8	52.1, get stuck

unstable behavior is due to the intrinsic phase lag between two wings or the gust wind during real flight [22].

D. Operation Principle and Process Parameter of Electrical-Discharge Wire Cutting [23]

The nontraditional EDWC methodology is similar to the electrical-discharge machining. This is a machining technique that, when in contact with the materials, discharges sparks. It uses electrical sparks to remove work-piece material. The spark melts a localized area of the original work piece and, in return, the leftover metal is what one wants. EDWC uses a very fine copper wire as electrode. The electrode wire adopted in the present work is made of brass and it has a diameter of 0.25 mm. The path of the wire travels from the supply spool, through the work piece, then onto a take-up spool. The work piece is held on a moveable table whose movements can be directed to create the desired shape for the work piece. The table movement is governed by computer-aided manufacture. Figure 4 is a schematic of an EDWC machining.

In this machining process, the work piece and the electrode wire are constantly flushed with deionized (DI) water at the machined area. DI water serves as a coolant as well as a medium for the current and it removes the metal debris or particles. The machining action

**Fig. 4** Schematic of operation of EDWC machining.

produces a working gap around the cutting wire. This gap usually ranges from 0.02 to 0.05 mm depending on the operating parameter. Once a test cut is made, the gap, which is uniform and repeatable, can be determined directly. With this manufacturing capability, EDWC can create precise parts down to just a few millimeters in size and has a margin tolerance of only 0.03 mm. Most important of all, the machining time is very short to several minutes for one contour cutting, and it is convenient to redesign the machining contour of the work piece. EDWC is actually beneficial to the fast prototyping of the small parts like the linkages and the holding bases of transmission modules of the MAVs in this work. The gear transmission module after the assembly of all small parts is shown in Fig. 5.

The leading-edge spar in Fig. 5 is made of 0.6-mm-diam carbon-fiber beams and it is connected to the aluminum-alloy third bars. A rib with 30 deg backswept to the leading-edge beam is optionally installed. All the tiny aluminum parts were precisely manufactured by EDWC and are listed in Table 2.

Table 2 shows that the mass of components machined by EDWC are greatly reduced with respect to other machining techniques. For instance, EDWC saves no less than 1.0 g on the parts of holding base and the second linkage bar. Because EDWC has good control, it can be used to make small gear parts out of aluminum-alloy 7075. This also allows using smaller steel pins to connect the Golden Snitch. Eagle II used larger brass pins. Because of this property, the resulting Golden Snitch is lighter. In fact, the transmission module by EDWC weights only 2.302 g, which is much lighter than 3.756 g of Eagle II and 2.8 g of Caltech's Microbat [24]. The new power transmission module made of aluminum alloy shown in Fig. 3 saves, at least, 1.454 g in weight. With the use of the EDWC technique, future MAVs can be made in a smaller and lighter scale.

In addition to the new gear transmission module, Golden Snitch also has a new pair of flexible wing frames. The goal is to keep reducing the body mass and wing span. The final design of the Golden Snitch has a wing span of 21.6 cm and a body mass of 5.9 g, and it is shown in Fig. 6. The body mass of 5.9 g of the Golden Snitch is composed of carbon-fiber leading-edge spar, parylene/polyethylene terephthalate wing skin, motor, gear transmission module, expandable polystyrene (EPS) fuselage, EPS tail, polylithium battery, and receiver.

To evaluate the mechanical power of the wing frames, the wing skin must be removed first. This mechanical testing looks at the power dissipation due to friction from the mechanical transmission. In this work, the friction dissipation of the Eagle II MAV accounts for 70% of the total electrical power, whereas in the modified Golden Snitch MAV it only consumes 45% of the total power. With the large decrease in weight and power loss, the wingbeat frequency of the Golden Snitch MAV can increase by 20 Hz or more.

III. Wind-Tunnel Testing of the Modified Flapping Golden Snitch MAV

Before the MAV takes on an actual flight, several tests are performed. The tests include a wind-tunnel testing and a flapping ground testing. In the flapping ground test, the flapping frequency or the wingbeat frequency ω is controlled by the dc motor and the

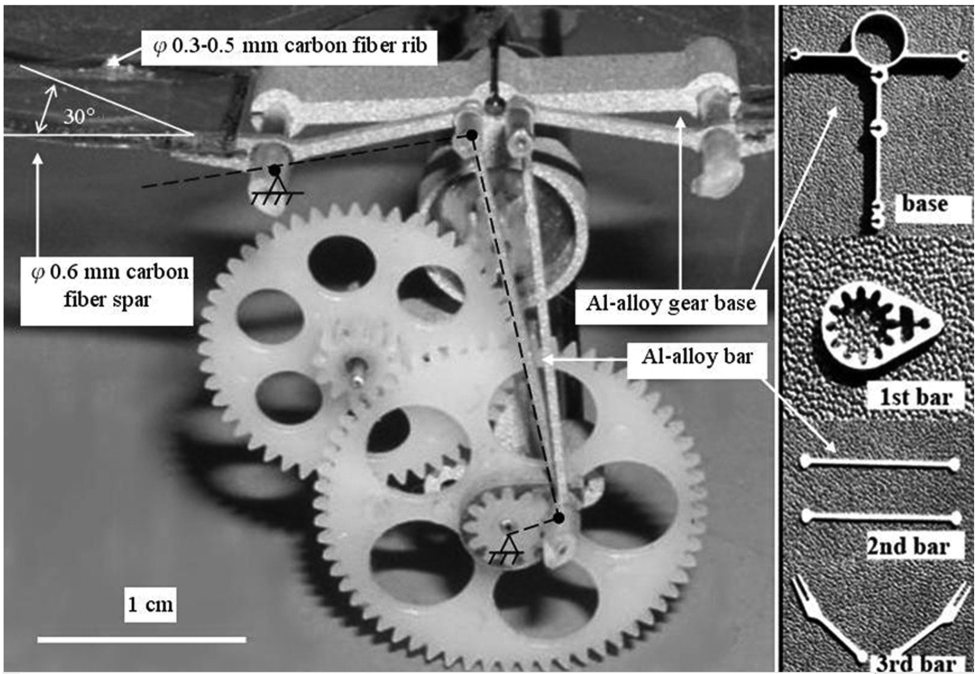





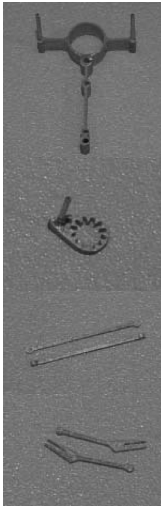
Fig. 5 Four-bar linkage (black dash line) gear transmission module [21] made by EDWC.

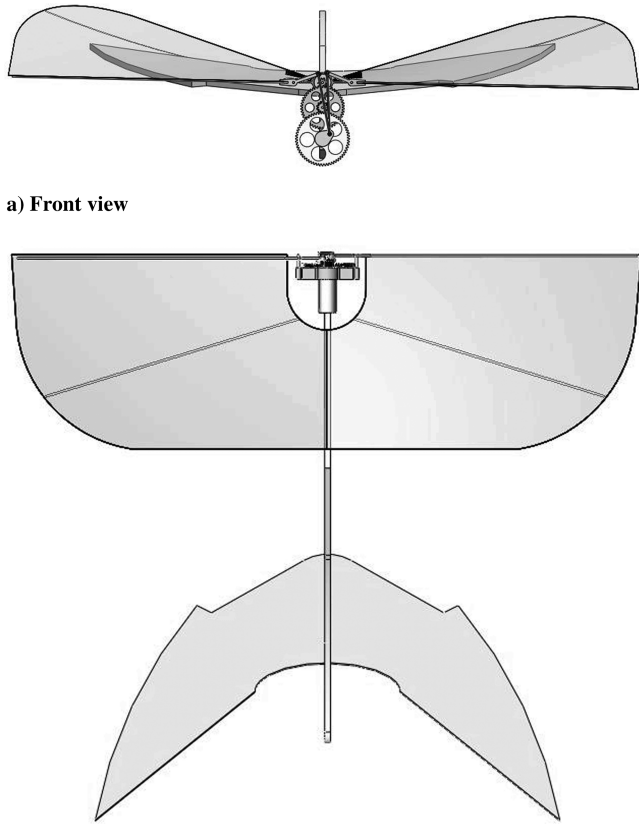
voltage applied to it. This dynamic test was conducted in a wind tunnel at the freestream speed U of 0.4–3.0 m/s, measured by a hot-wire anemometer. The load cell, with force specifications of 200 and 100 gf, is responsible for the force measurement of lift L and the net thrust ($T - D$), respectively. The margin of error is 0.2% of the full-scale signal due to nonlinearity or hysteresis. In the wind-tunnel test,

the MAV is installed on the load cell directly to obtain the data of lift and thrust forces.

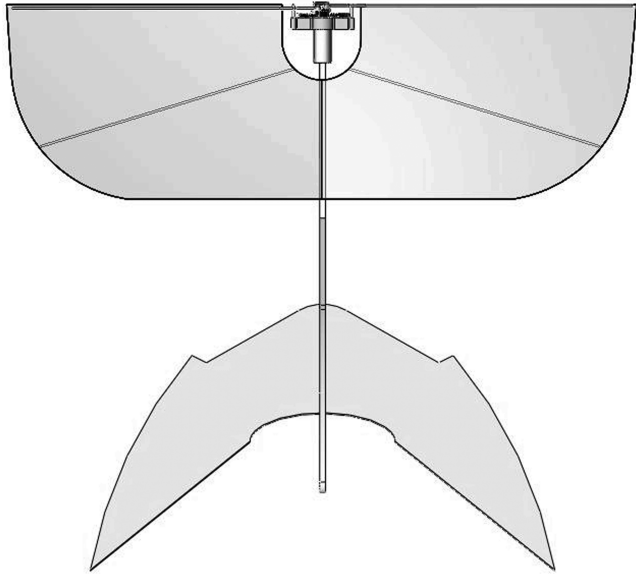
This unsteady aerodynamic investigation is quite different from the conventional case of steady aerodynamics. An important dimensionless parameter, namely the “advance ratio,” should be introduced here. The advance ratio J is defined as the ratio of the freestream velocity U to the maximum speed in the flapping direction. For

Table 2 Component mass for the gear transmission module with different processes and materials (masses reported in grams)

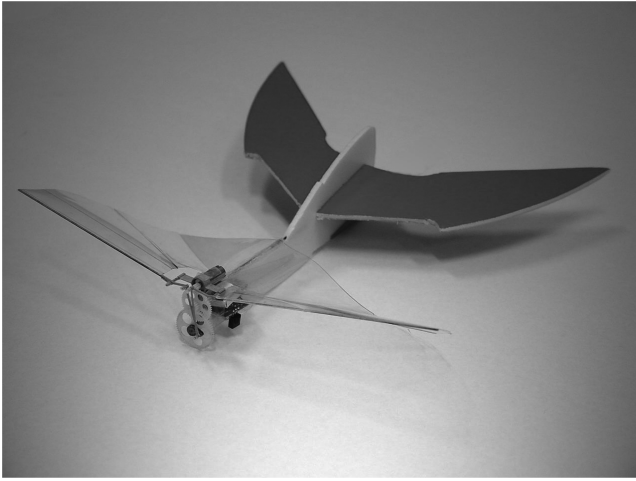
Parts	Figures	Eagle-II	Caltech's Microbat (by Pornsin-Sirirak [24])	Tamkang's Golden Snitch [21]
				
		Other techniques		EDWC
Holding base, no. 1		0.914, POM		0.261, Al-alloy 7075
First bar, part of no. 4		0.080, POM	Not available	0.030, Al-alloy 7075
Second bar, no. 5		0.362, bamboo		0.041, Al-alloy
Third bar, no. 6		0		0.040, Al-alloy
Others		0.484, brass		0.130, steel
	Connecting pins	1.450		1.400
	Electrical motor	0.373		0.373
	Gears, nos. 2–4	0.093		0.027
	Glue	3.756		2.302
Total mass			2.8	



a) Front view



b) Top view



c) The prototype [21]

Fig. 6 Golden Snitch MAV with wing area $S = 11,404 \text{ mm}^2$.

example, $J = U/b\omega\phi$, where the flapping speed is equal to the product of the wing span b , the wingbeat frequency ω , and the stroke angle ϕ . The J value approaches to a large number for the case of nonflapping wings; on the contrary, J is close to or less than one for the general unsteady flapping flight.

To analyze the wing-tunnel test, two variables are needed. One is the lift coefficient C_L and the other is the (net) thrust coefficient C_T . Both can be obtained by dividing the lift and the (net) thrust with the dynamic pressure force on the wing surface ($\rho U^2 S/2$). The actual instantaneous angle of attack (AOA) for the flapping flyers may be changed with time and it is not identical to the flapping inclined angle. Even high inclined angle of the flapping plane, for example, 50 deg, for the unsteady cases, still does not cause catastrophic flow separation. Rather, it induces better unsteady lift force by paying the

price of smaller thrust. This is the well-known effect called “delayed stall” [11,16].

The data-breeding rate of the load cell is set as 1000 points per second. The authors collected 12,000 points of 6-degree-of-freedom data including hundreds of flapping cycles for each test condition. These 12,000 points of data were averaged into one value for the lift L and one value for the net thrust ($T - D$), respectively. Figure 7 shows the lift coefficient of the Golden Snitch MAV without installing any tail on the MAV subject to the inclined angle (or AOA) of 20 deg. If the freestream velocity is 3 m/s, the dynamic pressure force on wing surface ($\rho U^2 S/2$), at standard atmosphere, is 6.415 gf, which is larger than the total weight, 5.9 gf, of the MAV. In other words, any flight condition with C_L higher than 0.92 in Fig. 7a has enough lift to overcome the MAV weight for actual flight.

IV. Flight Test

The goal is to fabricate a flapping MAV that can fly smoothly in the sky. However, before such goal can be achieved, the authors considered a simple indoors flight test of the Golden Snitch MAV. From the indoor test, the observed flight path and fuselage orientation reveal guidelines for MAV adjustments. Figure 8 shows the bad flying patterns that happened from the flight test. In Fig. 8a, for the pattern named “tail touchdown,” even with the full-power setting, the MAV flaps violently but sinks gradually. This happens because the MAV maintained a high AOA, which resulted in the tail touching the ground. This may be due to a heavier rear center of gravity or small stabilizer in the tail area. In Fig. 8b, for the pattern named “nose touchdown,” the MAV dives quickly and its nose touches the ground

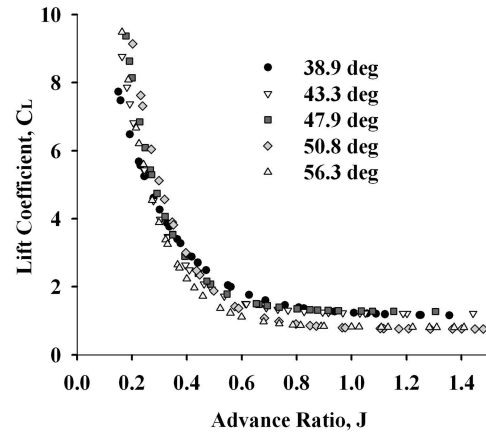
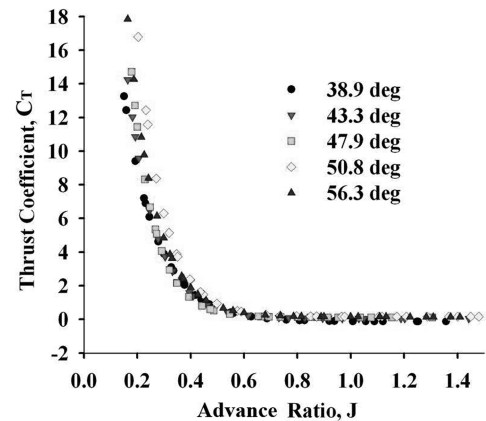
a) Lift coefficient C_L b) Thrust coefficient C_T

Fig. 7 Wind-tunnel data of Golden Snitch versus advance ratio J , corresponding to different stroke angles ϕ ($b = 21.6 \text{ cm}$, $\omega = 10.5\text{--}23.6 \text{ Hz}$).

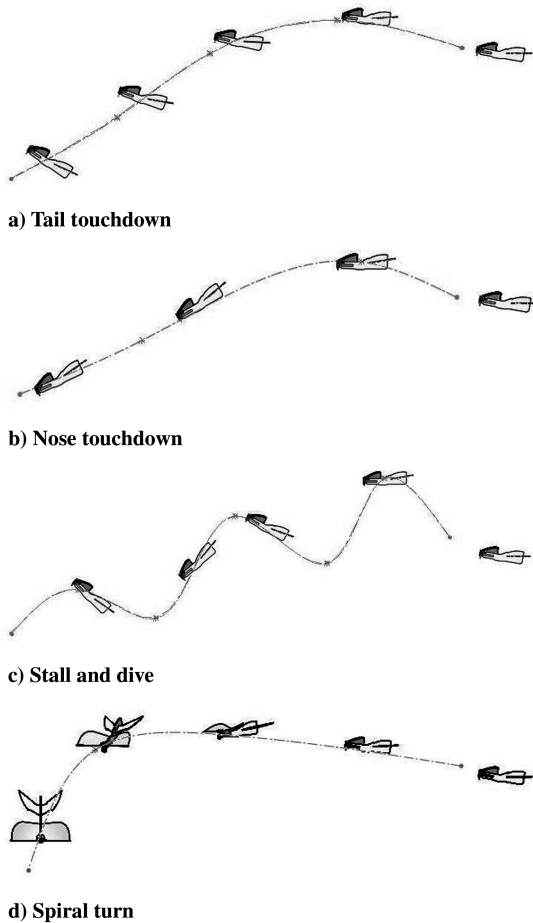


Fig. 8 Bad patterns of flight paths.

in a straightforward manner. The reason for such behavior may be due to insufficient pitch moment or heavy front center of gravity. In Fig. 8c, for the pattern named “stall and dive,” the MAV goes through a continuous stalling and diving, and finally lands with nose touching. This unstable flight is caused by large pitch moment. In Fig. 8d, for the flight path named “spiral turn,” the MAV flies forward a few meters, then turns instantly with a swift spiral trajectory to the ground. This is the most common and downcast problem. It may be caused by the different tension between the left and right wing. One can find the wrinkle on one side membrane of the flapping wings. Another issue is the big joint house at the third bar which brings an overloosened membrane in the flapping mode.

The new Golden Snitch MAV, equipped with the new configuration in Fig. 6 and characterized as lightweight and with high flexibility, has a far more outstanding flight performance than the semirigid Eagle II. With scarcely any real-time adjustment by remote control, the Golden Snitch actually achieved a successful flight record of 6 min 7 s on the Tamkang campus on 10 June 2009, breaking the 11 s record of the Eagle II to a great extent. The continuous snapshots of Golden Snitch during its real flight are shown in Fig. 9. Without the negative effect of side gust wind, Golden Snitch would like to soar roughly along the virtual barrel surface of an imaginary cylindrical column with the diameter of several meters if the tail generating negative lift is only used to stabilize the MAV.

Basically, Golden Snitch is vulnerable to the unpredictable outdoor environments, for example, the wind gust. Because of that, the maximum forward speed of Golden Snitch is only 3 m/s, comparable to the general tender side wind in outdoors but much less than the wind gust. Therefore, Golden Snitch is more suitable for indoor flight rather than outdoor flight.

Moreover, the control strategies which are important to the autonomous MAVs are still not clear in this stage. All the knowledge of controlling the wingbeat frequency of Golden Snitch is learned from the actual flight tests. For instance, the AOA or the inclined angle of Golden Snitch relates with the forward speed. In general, high forward speed only needs small AOA; high AOA is necessary to low forward speed.

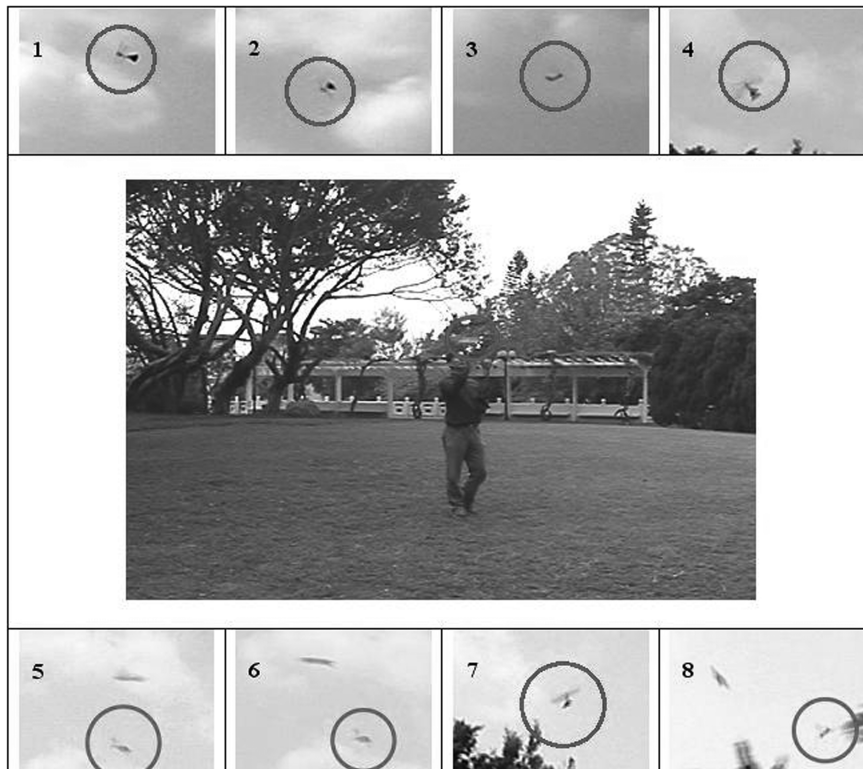


Fig. 9 Remote-controlled flight and the trajectory of the Golden Snitch MAV (http://tw.youtube.com/watch?v=YkEoxyWGI_k).

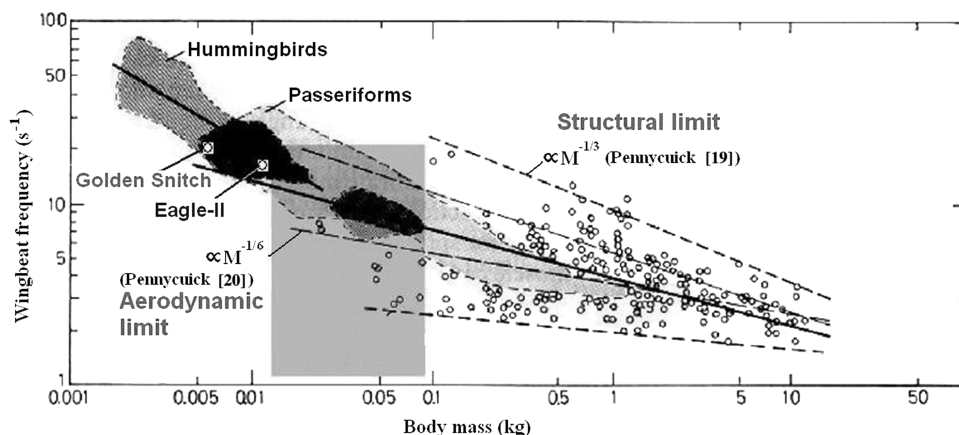


Fig. 10 Scaling laws for flapping flyers (see [15–20]) and the two MAVs in this work.

About the flight case of zero forward speed ($U = 0$), the authors must additionally admit that Golden Snitch with a single pair of wings is not capable of hovering. This is due to the weak lift hard for supporting the body mass during hovering. The authors actually performed a lift force measurement of Golden Snitch corresponding to different AOA subject to zero forward speed. (The lift data is not shown.) It reveals that the maximum lift of Golden Snitch at AOA = 80 deg is only 5.1 gf, less than Golden Snitch's weight of 5.9 gf. Therefore, the hovering flight herein is not feasible so far.

V. Comparison of Scaling Laws for Flapping Flyers

The denoted results of the Eagle II and Golden Snitch were inserted into Fig. 1, that is, the plot of wingbeat frequency versus body mass for flapping flyers, as in Fig. 10. The specifications for the Eagle II MAV are as follows: wing span = 30 cm, body mass = 11 g, and wingbeat frequency = 16 Hz. Whereas, the specifications for the Golden Snitch MAV are as follows: span = 21.6 cm, body mass = 5.9 g, and wingbeat frequency = 20 Hz. In Fig. 10, Golden Snitch is located to the left of Eagle II for the body mass result without degrading the wing loading. Such behavior agrees with the qualitative trend (1) \rightarrow (2), indicated in Fig. 1. The result provides a sense of encouragement for the continuing development of the new Golden Snitch MAV. The EDWC technique makes Golden Snitch possible. It helps to reduce the total body mass down to 5.9 g from the original 11 g.

VI. Conclusions

In conclusion, using the EDWC technique can reduce the body mass and improve the flight performance of flapping flyers. This work is the first time that such machining methodology is demonstrated in the development of a palm-size biomimetic MAV. Using EDWC, one can produce a lighter and more durable gear transmission module made of aluminum-alloy 7075 for the new MAV. This effectively reduces the body mass from 11 to 5.9 g and shrinks the wing span from 30 to 21.6 cm. The whole framework of design and manufacture for flapping MAVs herein not only keeps extending the MAV domain toward miniaturization, but also increases the flight endurance of the MAV to 6 min 7 s. The authors believe this implementation technique with the advantages of lightweight, small size, and time saving of manufacturing is promising in practice for the development of new flapping MAVs.

Acknowledgments

The authors are grateful to the financial support from National Science Council of Taiwan Government with the project no. NSC 96-2221-E-032-013/014 and 98-2221-E-032-025-MY3. The discussion with Y.-C. Tai of California Institute of Technology, and W.-P. Shih of National Taiwan University, Taiwan, is acknowledged.

In addition, the amendment to the technical writing by Betty T. Yang of Wright State University is also highly appreciated.

References

- [1] Żbikowski, R., "Fly Like a Fly," *IEEE Spectrum*, Vol. 42, No. 11, Nov. 2005, pp. 46–51.
doi:10.1109/MSPEC.2005.1526905
- [2] Pornsin-Sirirak, T. N., Tai, Y. C., Nassef, H., and Ho, C. M., "Titanium-Alloy MEMS Wing Technology for a Micro Aerial Vehicle Application," *Sensors and Actuators A: Physical*, Vol. 89, Nos. 1–2, 2001, pp. 95–103.
doi:10.1016/S0924-4247(00)00527-6
- [3] Barrett, R., McMurtry, R., Vos, R., Tiso, P., and De Breuker, R., "Post-Buckled Precompressed (PBP) Elements: A New Class of Flight Control Actuators Enhancing High-Speed Autonomous VTOL MAVs," *Proceedings of SPIE: The International Society for Optical Engineering*, Vol. 5762, Article No. 16, Bellingham, WA, 2005, pp. 111–122.
- [4] Jones, K. D., Bradshaw, C. J., Papadopoulos, J., and Platzter, M. F., "Bio-Inspired Design of Flapping-Wing Micro Aerial Vehicles," *Aeronautical Journal*, Vol. 109, No. 1098, 2005, pp. 385–393.
- [5] Rozhdestvensky, K. V., and Ryzhov, V. A., "Aerodynamics of Flapping-Wing Propulsors," *Progress in Aerospace Sciences*, Vol. 39, No. 8, 2003, pp. 585–633.
doi:10.1016/S0376-0421(03)00077-0
- [6] Banala, S. K., and Agrawal, S. K., "Design and Optimization of a Mechanism for Out-of-Plane Insect Winglike Motion with Twist," *Journal of Mechanical Design*, Vol. 127, No. 4, 2005, pp. 841–844.
doi:10.1115/1.1924474
- [7] McIntosh, S. H., Agrawal, S. K., and Khan, Z., "Design of a Mechanism for Biaxial Rotation of a Wing for a Hovering Vehicle," *IEEE/ASME Transactions on Mechatronics*, Vol. 11, No. 2, 2006, pp. 145–153.
doi:10.1109/TMECH.2006.871089
- [8] Żbikowski, R., Galiński, C., and Pedersen, C. B., "Four-Bar Linkage Mechanism for Insectlike Flapping Wings in Hover: Concept and an Outline of Its Realization," *Journal of Mechanical Design*, Vol. 127, No. 4, 2005, pp. 817–824.
doi:10.1115/1.1829091
- [9] Żbikowski, R., and Galiński, C., "Insect-Like Flapping Wing Mechanism Based on a Double Spherical Scotch Yoke," *Journal of the Royal Society Interface*, Vol. 2, No. 3, 2005, pp. 223–235.
doi:10.1098/rsif.2005.0031
- [10] Yang, L. J., Hsu, C. K., Ho, J. Y., and Feng, C. K., "Flapping Wings with PVDF Sensors to Modify the Aerodynamic Forces of a Micro Aerial Vehicle," *Sensors and Actuators A: Physical*, Vol. 139, Nos. 1–2, 2007, pp. 95–103.
doi:10.1016/j.sna.2007.03.026
- [11] Dickinson, M. H., Lehmann, F. O., and Sane, S. P., "Wing Rotation and the Aerodynamic Basis of Insect Flight," *Science*, Vol. 284, No. 5422, 1999, pp. 1954–1960.
doi:10.1126/science.284.5422.1954
- [12] Srygley, R. B., and Thomas, A. L. R., "Unconventional Lift-Generating Mechanisms in Free-Flying Butterflies," *Nature*, Vol. 420, No. 6916, 2002, pp. 660–664.

- doi:10.1038/nature01223
- [13] Sun, Y., and Nelson, B. J., "MEMS Capacitive Force Sensors for Cellular and Flight Biomechanics," *Biomedical Materials*, Vol. 2, No. 1, 2007, pp. s16–s22.
 - [14] Hedenström, A., Johansson, L. C., Wolf, M., Von Busse, R., Winter, Y., and Spedding, G. R., "Bat Flight Generates Complex Aerodynamic Tracks," *Science*, Vol. 316, No. 5826, 2007, pp. 894–897. doi:10.1126/science.1142281
 - [15] Ho, S., Nassef, H., Pornsinsirak, N., Tai, Y.-C., and Ho, C.-M., "Unsteady Aerodynamics and Flow Control for Flapping Wing Flyers," *Progress in Aerospace Sciences*, Vol. 39, No. 8, 2003, pp. 635–681. doi:10.1016/j.paerosci.2003.04.001
 - [16] Norberg, U. M., *Vertebrate Flight: Mechanics, Physiology, Morphology, Ecology and Evolution*, Springer, New York, 1990, pp. 39, 103, 167–181.
 - [17] Greenewalt, C. H., "The Flight of Birds," *Transactions of the American Philosophical Society*, Vol. 65, No. 4, 1975, pp. 1–67. doi:10.2307/1006161
 - [18] Shyy, W., Berg, M., and Ljungqvist, D., "Flapping and Flexible Wings for Biological and Micro Air Vehicles," *Progress in Aerospace Sciences*, Vol. 35, No. 5, 1999, pp. 455–505. doi:10.1016/S0376-0421(98)00016-5
 - [19] Pennycuik, C. J., "Mechanical Constraints on the Evolution of Flight," *The Origin of Birds and the Evolution of Flight*, edited by K. Padian, Vol. 8, California Academy of Science, San Francisco, 1986, pp. 83–98.
 - [20] Pennycuik, C. J., "Mechanics of Flight," *Avian Biology*, edited by D. S. Farner, and J. R. King, Vol. 5, Academic Press, London, 1975, pp. 1–75.
 - [21] Yang, L.-J., Hsu, C.-K., Hsiao, F.-Y., Shen, Y.-K., and Feng, C.-K., "A Micro-Aerial-Vehicle (MAV) with Figure-of-Eight Flapping Induced by Flexible Wing Frames," AIAA Paper 2009-0875, Jan. 2009.
 - [22] Young, W.-B., "The Thrust and Lift of an Ornithopter's Membrane Wings with Simple Flapping Motion," *Aerospace Science and Technology*, Vol. 10, No. 2, 2006, pp. 111–119. doi:10.1016/j.ast.2005.10.003
 - [23] Weller, E. J., *Nontraditional Machining Processes*, Second Ed., The Society of Manufacturing Engineers, Dearborn, MI, 1984, pp. 162–170.
 - [24] Pornsin-Sirirak, T. N., "Parylene MEMS Technology for Adaptive Flow Control of Flapping Flight," Ph.D. Dissertation, Electrical Engineering, California Inst. of Technology, Pasadena, Jan. 2002.